Chemical Physics 173 (1993) 421–437
North-Holland

# Theoretical study of the electronic spectra of a polycyclic aromatic hydrocarbon, naphthalene, and its derivatives

Ping Du [a,1], Farid Salama [b] and Gilda H. Loew [a]

[a] *Molecular Research Institute, 845 Page Mill Road, Palo Alto, CA 94304, USA*
[b] *NASA–Ames Research Center, MS: 245-6, Space Science Division, Moffett Field, CA 94035-1000, USA*

Received 25 November 1992

In order to preselect possible candidates for the origin of diffuse interstellar bands observed, semiempirical quantum mechanical method INDO/S was applied to the optical spectra of neutral, cationic, and anionic states of naphthalene and its hydrogen abstraction and addition derivatives. Comparison with experiment shows that the spectra of naphthalene and its ions were reliably predicted. The configuration interaction calculations with single-electron excitations provided reasonable excited state wavefunctions compared to ab initio calculations that included higher excitations. The degree of similarity of the predicted spectra of the hydrogen abstraction and derivatives to those of naphthalene and ions depends largely on the similarity of the $\pi$ electron configurations. For the hydrogen addition derivatives, very little resemblance of the predicted spectra to naphthalene was found because of the disruption of the aromatic conjugation system. The relevance of these calculations to astrophysical issues is discussed within the context of these polycyclic aromatic hydrocarbon models. Comparing the calculated electronic energies to the diffuse interstellar bands (DIBs), a list of possible candidates of naphthalene derivatives is established which provides selected candidates for a definitive test through laboratory studies.

## 1. Introduction

Polycyclic aromatic hydrocarbons (PAHs) have been postulated as important interstellar constituents both in free form, where they are the most abundant interstellar organic molecules known, and as the building blocks of interstellar dust [1–4]. These molecules in their ionized and/or neutral forms are thought to be the origin of a variety of interstellar infrared emission features observed in the 700 to 3100 $cm^{-1}$ range. The main hypothesis in the model dealing with the infrared emission is that PAHs probably present as a mixture of positive ions and some radicals as well as neutral species are responsible for most of the discrete infrared emission bands through ultraviolet-pumped infrared fluorescence in a collision-free environment.

Moreover, the ubiquitous presence of ionized PAHs in the interstellar medium makes them very attractive candidates for the diffuse interstellar absorption bands (DIBs) [5]. DIBs number now more than a hundred, and extend from about 23000 $cm^{-1}$ (4400 Å) to the near infrared [6].

While PAHs have been postulated as an important interstellar constituent on the basis of the IR emission spectra, the ultraviolet, visible, and near-infrared absorption properties of the free, unperturbed species, which are required to understand the radiation and energy balance in space, are not known. This has motivated our semi-empirical quantum mechanical calculations of the electronic structure and spectra of the smallest member of PAHs, i.e. naphthalene and its derivatives.

Numerous spectroscopic studies on naphthalene clusters and its radical ions have been carried out in salt media [7–9]. However, the electronic spectra of the trapped species were strongly perturbed by the ionic solvent. A recent study focuses on the spectroscopy of naphthalene and its ions truly isolated in low-temperature inert gas matrices where the perturbation of the solvent to the species under study is minimum and the environment more relevant to astrophysical applications [10,11]. Theoretical studies of neutral naphthalene [12] were facilitated by the well-

[1] To whom correspondence should be addressed.

focused assumption that the entire spectrum is derived from excitations within the π electron system. Procedures such as the PPP and CNDO/S methods resulted in predictions that were in good agreement with experiments. These studies also predicted most of the absorption bands of the naphthalene cation [13,14] and anion [15–20]. However, neither experimental nor theoretical study of the hydrogen abstraction and addition derivatives have been reported.

Thus, we have calculated the electronic structure and spectra of these naphthalene radical species in their neutral, cationic and anionic forms. In order to validate the methods used, we have repeated calculations for naphthalene and its anion and cation, and compared them with experimental results and previous theoretical calculations.

In a recent study [11], it was found that a small number of DIBs (six in all) coincide with bands of the naphthalene cation and that a mixture of different PAHs and their derivatives may well explain some of the DIBs. Thus, the main goal of this work was to provide theoretical analyses of the calculated spectra for comparisons with available experimental measurements and also to provide specific candidates among the various possible isomers for laboratory studies and comparison with astronomical observations of the DIBs.

## 2. Methods

To assess the method used for geometry optimization, various semiempirical techniques were used for naphthalene by using the program MOPAC [21]. AM1 [22], which gave the optimized geometry of naphthalene closest to experiment, was used for the optimization of neutral naphthalene radicals resulting from H atom abstraction or addition. There are four such radicals: $C_{10}H_7$-$\alpha^{\cdot}$, $C_{10}H_7$-$\beta^{\cdot}$, $C_{10}H_9$-$\alpha^{\cdot}$ and $C_{10}H_9$-$\beta^{\cdot}$ ($\alpha$ and $\beta$ denote the positions where the hydrogen atom is abstracted or added). $C_s$ symmetry was imposed during the optimization. Since hydrogen addition destroys the aromaticity of naphthalene π system, vibrational analyses were performed on the optimized geometries of $C_{10}H_9$-$\alpha^{\cdot}$ and $C_{10}H_9$-$\beta^{\cdot}$ to verify the geometries obtained to be true energy minima. Energy and spectra calculations were carried out by using the semiempirical INDO/S method [23].

## 3. Results

As shown in table 1, AM1 and PM3 gave bond lengths of naphthalene closest to the average of the experimentally determined values, as deduced by Pauling [24]. Thus, AM1 was used for optimizing the geometries of naphthalene derivatives. The optimized geometries of the four neutral radicals are shown in fig. 1. *The geometries of the hydrogen atom addition derivatives are not distorted from planarity and are true energy minima since all vibrational frequencies were found to be real.*

The π MO energy levels of naphthalene and its cation and anion are shown in fig. 2. In the two radicals resulting from hydrogen abstraction, the $^2A'$ state was found to be the ground state, in which the unpaired electron occupies the nonbonding $sp^2$ orbital (σ) localized at the dehydrogenated carbon atom. The $^2A''$ states with the σ orbital doubly occupied and the $\pi_5$ orbital singly occupied were calculated to be 52.9 and 56.2 kcal/mol higher in energy for $C_{10}H_7$-$\alpha$ and $C_{10}H_7$-$\beta$ respectively. In the two radicals resulting from hydrogen atom addition the unpaired electron in the $^2A''$ ground state occupies the $\pi_5$ orbital. Since

Table 1
Comparison of optimized bond lengths of naphthalene using different methods

| | AM1 | MINDO/3 | MNDO | PM3 | Exp. [a] |
|---|---|---|---|---|---|
| $r_{C-C'}$ [b] | 1.416 | 1.430 | 1.429 | 1.415 | 1.401 |
| $r_{C-C\alpha}$ | 1.373 | 1.380 | 1.382 | 1.369 | 1.372 |
| $r_{C\alpha-C\beta}$ | 1.422 | 1.449 | 1.439 | 1.421 | 1.422 |
| $r_{C\beta-C\beta'}$ | 1.419 | 1.462 | 1.435 | 1.410 | 1.412 |

[a] Ref. [24].
[b] The carbon atoms bridging the two rings are labeled as C and C'.

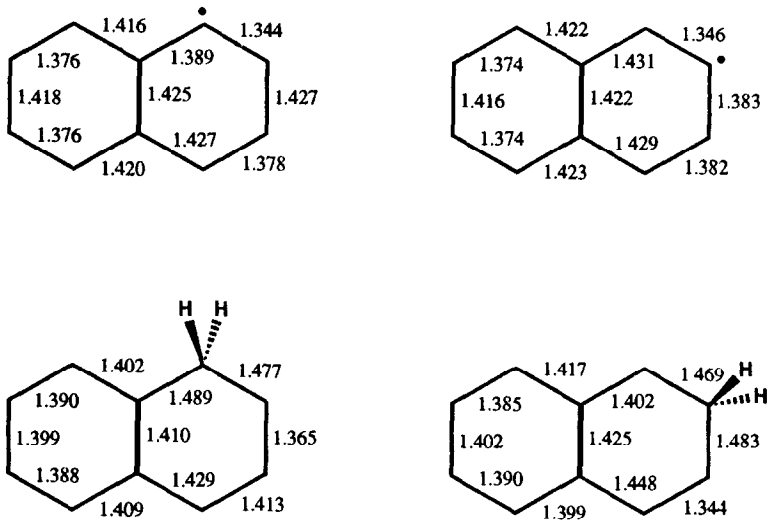


Fig. 1. Optimized geometries of the hydrogen abstraction and addition derivatives of naphthalene.

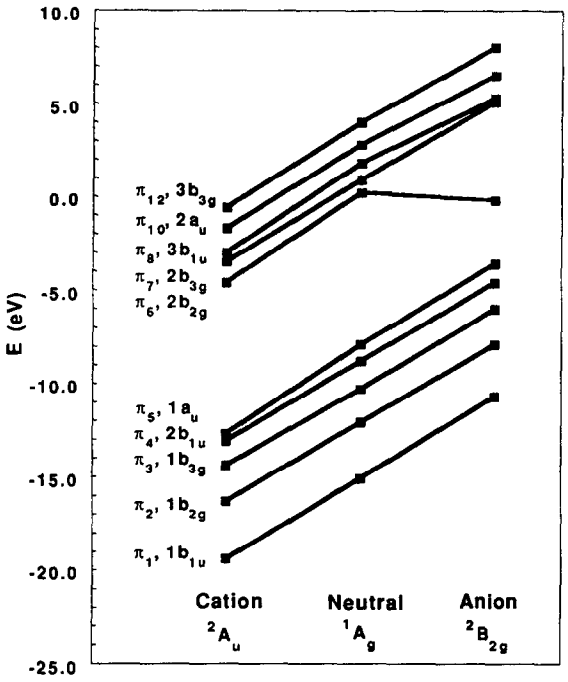


Fig. 2. π MO energy diagram of naphthalene and its ions.

there are no near degenerate orbitals in these radical species, the $^2A''$ states were assumed to be the ground states.

For the cations and anions of the dehydrogenated species of naphthalene, there are three low-lying states, $^3A''$, $^1A''$, and $^1A'$ formed by different orbital occupancies and spin couplings. For the cations, the $^3A''$ and $^1A''$ states have two electrons occupying the $\pi_5$ and σ orbitals. The $^1A'$ state is resulted primarily from the configuration with both electrons occupying the $\pi_5$ orbital mixed in with a second configuration with the two electrons occupying the σ orbital.

To determine the ground states of these ionic derivatives, SCF and limited CISD (configuration interaction with single and double excitations) calculations were carried out. In the SCF calculations, the state energies were calculated by converging the molecular orbitals of each state to a single electron configuration. For the CISD calculations, a set of MOs that are unbiased to either the singlet or the triplet state were first obtained by applying the configuration-averaged Hartree–Fock procedure [25] over the three low-lying states resulting from two electrons distributing in the two orbitals (σ and $\pi_5$ for the cation and σ and $\pi_6$ for the anion). CISD calculations were then performed for each of the low-lying states. Three reference configurations, $|...\pi^2\sigma^0\rangle$, $|...\pi^1\sigma^1\rangle$, and $|...\pi^0\sigma^2\rangle$, where π is $\pi_5$ for the cations and $\pi_6$ for the anions, were included for all three states. Using the set of average MOs and the three reference configurations, excitations of singles and doubles were allowed within a set of nine orbitals, including eight

$\pi$ ($\pi_2$–$\pi_9$) and one nonbonding ($\sigma$) orbitals.

The determination of the ground states of the cations and anions of the H-atom addition derivatives $C_{10}H_9$-$\alpha^+$, $C_{10}H_9$-$\beta^+$, $C_{10}H_9$-$\alpha^-$ and $C_{10}H_9$-$\beta^-$ was more straightforward than the ionic species of the H-abstracted naphthalenes. Since the unpaired electron occupies the $\pi_5$ orbital in the $^2A''$ ground state of the neutral compound, the most stable anion is formed by the addition of an electron to that orbital and the most stable cation by extracting an electron from that orbital, leading in both cases to $^1A'$ states.

The electron occupancies and the relative energies of the three low-lying states of the hydrogen abstracted ions calculated at both the SCF and CISD levels are listed in table 2. The relative energies calculated with CISD, which takes account of excited configurations that mix into the single electron configurations, are similar to the ROHF results. At both levels, $^3A''$ and $^1A'$ were calculated to be the ground states of the cations and the anions, respectively. In summary, the electron occupancies for the ground states of the 15 naphthalene derivatives are shown in table 3.

Singles only configuration interaction (CIS) using the INDO approximation has been shown to accurately reproduce the optical spectra of neutral naphthalene [26] and other PAHs [27]. In this study, the CIS spectra calculations for naphthalene derivatives include excitations within the full valence MO set for naphthalene and its anion and cation. For the hydrogen abstraction and addition derivatives of naphthalene, excitations within 10 $\pi$ orbitals and about 15 $\sigma$ orbitals are included. The optimized geometries of the neutral species were used for the spectral calculations of the neutral as well as the corresponding ionic states.

The calculated spectra of all compounds are shown in figs. 3a–3o. In addition, the spectra of naphthalene and its cation and anion calculated at the experimental geometry of naphthalene [24], are compared with experiments and previous calculations in tables 4–6. The dominant configurations of the excited states are also listed in the tables in detail. Tables 7–18 show the calculated spectra of naphthalene derivatives. Only those transitions with $\leqslant 40\,000$ cm$^{-1}$ are included in these tables.

## 4. Discussions of computational results

As shown in table 2, both hydrogen abstracted naphthalene cations are found to have a triplet ground state, $^3A''$. The open shell singlet state, $^1A''$, is higher in energy at the ROHF level, consistent with Hund's rule. Inclusion of electron correlations in the CISD calculations in the complete $\pi$ space increases the relative energies of $^1A''$ by about 2 kcal/mol. The closed shell singlet state, $^1A'$, was found to be the highest in energy at both ROHF and CISD levels.

By contrast, for both anions of the hydrogen abstraction derivatives, the closed shell singlet state, $^1A'$, was calculated to be the ground state because of the high orbital energy of $\pi_6$. At both the ROHF and CISD levels, the triplet state was found to be higher in energy. The relative energies of the open shell singlet states are the highest and increase from the ROHF

Table 2
Relative energies of the low-lying states of $C_{10}H_7$ formed by H atom abstraction from naphthalene

| Charge | State | Configuration | $-H_\alpha$ | | $-H_\beta$ | |
|---|---|---|---|---|---|---|
| | | | ROHF | CISD [a] | ROHF | CISD [a] |
| +1 | $^1A'$ | $\pi_1^2\pi_2^2\pi_3^2\pi_4^2\pi_5^2\sigma^0$ | 12.7 | 12.5 | 12.4 | 12.4 |
| | $^1A''$ | $\pi_1^2\pi_2^2\pi_3^2\pi_4^2\pi_5^1\sigma^1$ | 5.3 | 7.8 | 2.6 | 4.0 |
| | $^3A''$ | $\pi_1^2\pi_2^2\pi_3^2\pi_4^2\pi_5^1\sigma^1$ | 0.0 | 0.0 | 0.0 | 0.0 |
| −1 | $^1A'$ | $\pi_1^2\pi_2^2\pi_3^2\pi_4^2\pi_5^2\pi_6^0\sigma^2$ | 0.0 | 0.0 | 0.0 | 0.0 |
| | $^1A''$ | $\pi_1^2\pi_2^2\pi_3^2\pi_4^2\pi_5^2\pi_6^1\sigma^1$ | 8.7 | 14.8 | 6.1 | 7.2 |
| | $^3A''$ | $\pi_1^2\pi_2^2\pi_3^2\pi_4^2\pi_5^1\pi_6^1\sigma^1$ | 5.3 | 6.1 | 4.2 | 4.0 |

[a] CISD included 8 MOs, 8 electrons, and 3 reference configurations: $|...\pi^1\sigma^1\rangle$, $|...\pi^2\sigma^0\rangle$, $|...\pi^0\sigma^2\rangle$. MOs were converged to an average multiplicity.

Table 3
Ground state electron occupancies of naphthalene derivatives

| | Cation | Neutral | Anion |
|---|---|---|---|
| naphthalene | $^2A_u(...\pi_4^2\pi_5^1)$ | $^1A_g(...\pi_4^2\pi_5^2)$ | $^2B_{2g}(...\pi_4^2\pi_5^2\pi_6^1)$ |
| $-H_\alpha$ | $^3A''(...\pi_4^2\pi_5^1\sigma^1)$ | $^2A'(...\pi_4^2\pi_5^2\sigma^1)$ | $^1A'(...\pi_4^2\pi_5^2\sigma^2)$ |
| $-H_\beta$ | $^3A''(...\pi_4^2\pi_5^1\sigma^1)$ | $^2A'(...\pi_4^2\pi_5^2\sigma^1)$ | $^1A'(...\pi_4^2\pi_5^2\sigma^2)$ |
| $+H_\alpha$ | $^1A'(...\pi_4^2\pi_5^0)$ | $^2A''(...\pi_4^2\pi_5^1)$ | $^1A'(...\pi_4^2\pi_5^2)$ |
| $+H_\beta$ | $^1A'(...\pi_4^2\pi_5^0)$ | $^2A''(...\pi_4^2\pi_5^1)$ | $^1A'(...\pi_4^2\pi_5^2)$ |

level to the CISD level, in parallel with the results calculated for the cations (table 2).

Comparing with experiments [28,29], the calculated spectra of neutral naphthalene and its ions demonstrate the reliability of the INDO/S method in predicting the electronic spectra of PAHs (table 4). Four allowed transitions $1\,^1B_{3u}$, $1\,^1B_{2u}$, $2\,^1B_{3u}$, and $2\,^1B_{2u}$, were found for naphthalene, with the calculated oscillator strengths in agreement with the experimental data. The calculated excitation energy for the first absorption (32.3 kK), $1\,^1B_{3u}$, agree with experiments almost exactly. The energy for the second state (33.9 kK), $1\,^1B_{2u}$, also agrees with experiment very well, only 2 kK lower than the experimental value taken in the neon matrix [10]. For the higher energy states, the agreements are not as good and the excitation energies were underestimated by as much as 4 kK. However, compared to typical ab initio calculations that ignores correlation of σ electrons [30], the current results are significantly better in predicting excitation energies, as demonstrated by other semiempirical studies [12].

Although only single excitations were included in CIS, the dominant configurations of each excited state of naphthalene are similar to those found in calculations with higher excitations included [30], indicating similar qualitative descriptions of these excited states. However, the contributions of these dominant configurations are probably over estimated because of the omission of excitations of doubles and higher. In this study, two main excitations, $1a_u \rightarrow 2b_{3g}$ and $2b_{1u} \rightarrow 2b_{2g}$, were found for the first excited state, $1\,^1B_{3u}$, with about half to half out-of-phase combination. The first excitation is from the highest occupied orbital to the second lowest unoccupied orbital and the second excitation is from the second highest occupied orbital to the lowest unoccupied orbital. As shown in the orbital energy diagram (fig. 2), these two excitations require about the same energy and thus mix almost equally. The small oscillator strength for $1\,^1B_{3u}$ and large oscillator strength for $2\,^1B_{3u}$ are a result of this mixing, as illustrated by Hoijtink et al. [19]. By contrast, the two dominant configurations of $1\,^1B_{2u}$ and $2\,^1B_{2u}$, $1a_u \rightarrow 2b_{2g}$ and $2b_{2u} \rightarrow 2b_{3g}$, require different energies and these two states have oscillator strengths closer to each other.

For the symmetry forbidden transitions, the INDO/S energies are lower than the ab initio energies but the dominant configurations are mostly the same, similar to those states of allowed transitions (table 4). One state, $1\,^1B_{3g}$ involving excitations to a $\sigma^*$ orbital, was also found near 50 kK.

Similar accuracies were obtained for the calculated spectra of naphthalene cation and anion compared to experiments (tables 5 and 6). Although the calculated oscillator strengths for the cation spectrum show discrepancies with the experimental values obtained in the neon matrix [10], they are in good agreement with the measurements in the freon matrix [16] and polarized spectra [17]. Compared to the existing theoretical results on the naphthalene cation and anion using other semiempirical methods [13–15], these predicted spectra are slightly more accurate and more complete. In addition to the transitions corresponding to the four excited states of naphthalene, more lower-energy excitations were found for the cation and the anion. The extra bands result from the excitations to the half filled orbitals, $1a_u$ for the cation and $2b_{2g}$ for the anion. For the anion, two weak transitions mostly resulting from $\pi \rightarrow \sigma^*$ were also found to be near 30 and 42.2 kK respectively. The oscillator strengths of these transitions were found to be small, in agreement with experiment.

Good agreement of the spectra calculated for naphthalene and its cation and anion with experiment allowed us to extend the INDO/S method to

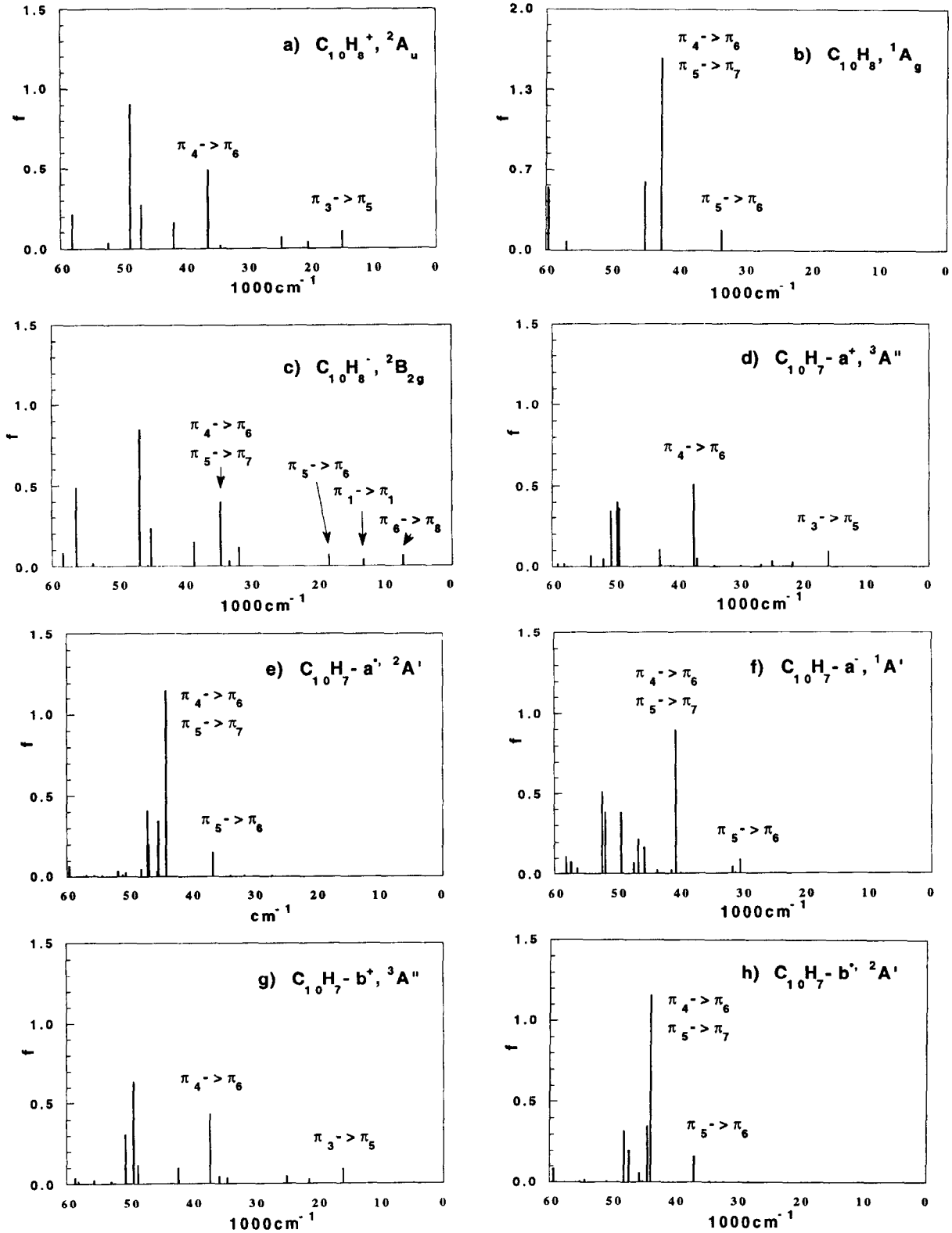


Fig. 3. Calculated electronic spectra of neutral and ionic species of naphthalene and its hydrogen abstraction and addition derivatives.

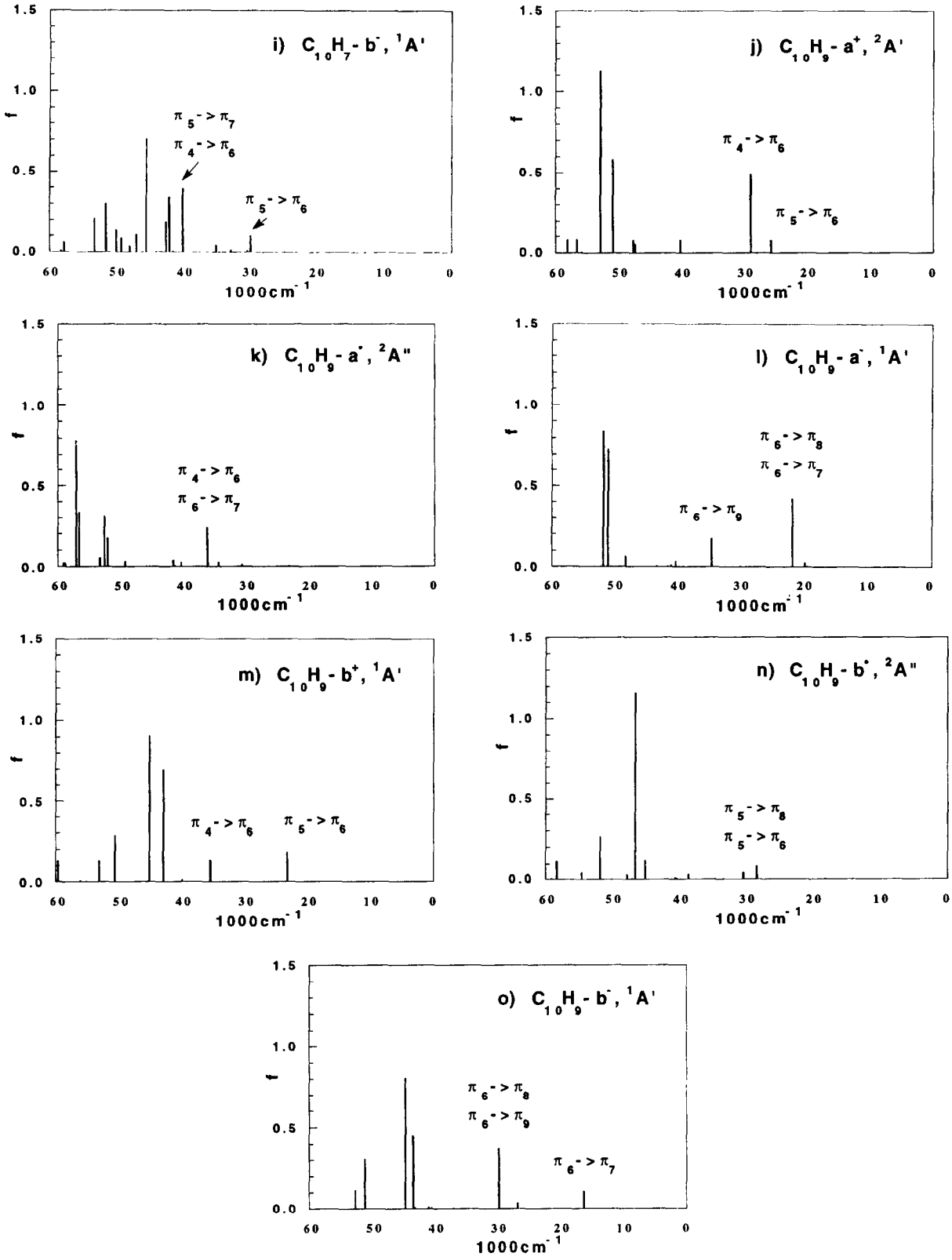


Fig. 3. Continued

Table 4
INDO/S-CI calculated excited states of neutral naphthalene (energy in 1000 $cm^{-1}$)

| State | Polarization | This work [a] | | | Ab initio calculation [b] | | | Experiment | | |
|---|---|---|---|---|---|---|---|---|---|---|
| | | Configuration | $c^2$ | $\Delta E(f)$ | Configuration | $c^2$ | $\Delta E(f)$ | $\Delta E(f)$ [c] | $\Delta E(f)$ [d] | $\Delta E(f)$ [e] |
| $1\,^1A_g$ | | HF | 1.00 | 0.0 | HF | 0.82 | 0.0 | | | |
| $1\,^1B_{3u}$ | $x$ | $1a_u \rightarrow 2b_{3g}$ | 0.54 | 32.3(0.003) | $1a_u \rightarrow 2b_{3g}$ | 0.34 | 36.3(0.001) | 32.1(0.07) | 32.2(0.001) | 32.0(0.002) |
| | | $2b_{1u} \rightarrow 2b_{2g}$ | 0.43 | | $2b_{1u} \rightarrow 2b_{2g}$ | 0.38 | | | | |
| $1\,^1B_{2u}$ | $y$ | $1a_u \rightarrow 2b_{2g}$ | 0.86 | 33.9(0.166) | $1a_u \rightarrow 2b_{2g}$ | 0.77 | 54.0(0.100) | 35.8(0.13) | 35.9(0.11) | 35.9(0.102) |
| | | $2b_{1u} \rightarrow 2b_{3g}$ | 0.11 | | $2b_{1u} \rightarrow 2b_{3g}$ | 0.09 | | | | |
| $2\,^1B_{3u}$ | $x$ | $2b_{1u} \rightarrow 2b_{2g}$ | 0.54 | 42.8(1.590) | $2b_{1u} \rightarrow 2b_{2g}$ | 0.42 | 66.1(1.94) | 47.3(1.72) | 47.5(1.3) | 48.4(1.3) |
| | | $1a_u \rightarrow 2b_{3g}$ | 0.42 | | $1a_u \rightarrow 2b_{3g}$ | 0.41 | | | | |
| $1\,^1B_{1g}$ | | $1a_u \rightarrow 3b_{1u}$ | 0.92 | 42.9 | $1a_u \rightarrow 3b_{1u}$ | 0.30 | 55.6 | | | |
| | | | | | $1b_{3g} \rightarrow 2b_{2g}$ | 0.26 | | | | |
| $2\,^1A_g$ | | $2b_{1u} \rightarrow 3b_{1u}$ | 0.61 | 44.5 | $2b_{1u} \rightarrow 3b_{1u}$ | 0.31 | 48.4 | | | |
| | | $1b_{3g} \rightarrow 2b_{3g}$ | 0.22 | | $1b_{3g} \rightarrow 2b_{3g}$ | 0.27 | | | | |
| $2\,^1B_{2u}$ | $y$ | $2b_{1u} \rightarrow 2b_{3g}$ | 0.83 | 45.3(0.563) | $2b_{1u} \rightarrow 2b_{3g}$ | 0.42 | 64.5(0.50) | 49.1(0.60) | 52.6 | 49.5(0.3) |
| | | $1a_u \rightarrow 2b_{2g}$ | 0.11 | | $1a_u \rightarrow 2b_{2g}$ | 0.41 | | | | |
| $1\,^1B_{3g}$ | | $1a_u \rightarrow 5b_{2u}(\sigma^*)$ | 0.94 | 49.3 | – | | – | | | |
| $2\,^1B_{1g}$ | | $1b_{3g} \rightarrow 2b_{2g}$ | 0.93 | 49.5 | $1b_{2g} \rightarrow 2b_{3g}$ | 0.22 | 62.9 | | | |
| | | | | | $2b_{1u}1a_u \rightarrow 2b_{3g}2b_{3g}$ | 0.13 | | | | |
| | | | | | $2b_{1u} \rightarrow 2a_u$ | 0.12 | | | | |
| | | | | | $1a_u \rightarrow 2b_{2g}$ | 0.41 | | | | |

[a] CIS includes full 48 MOs of the ground state $^1A_g$ calculated with RHF-SCF.
[b] CASSCF, Matos and Roos, ref. [27].
[c] Neon matrix, Salama and Allamandola, ref. [10].
[d] Energy-loss (vapor), Huebner et al., ref. [28].
[e] Absorption (vapor), George and Morris, ref. [29].

the prediction of the spectra for the twelve uncharacterized naphthalene derivatives, the hydrogen abstraction and addition compounds and their cationic and anionic forms. The calculated spectra, together with those of naphthalene and its cation and anion, are plotted in figs. 3a–3o.

Some general similarities and differences can be found among the calculated spectra of these hydrogen abstraction and addition derivatives. *Similar spectra are found for derivatives with the same π electron configurations.* For example, the cations of both hydrogen abstracted derivatives, $C_{10}H_7$-$\alpha^+$ and $C_{10}H_7$-$\beta^+$, have similar excited state profiles as naphthalene cation. They all include a weak transition to the half filled $\pi_5$ orbital near 16 kK, $\pi_3 \rightarrow \pi_5$, and a moderately strong transition near 37 kK, $\pi_4 \rightarrow \pi_6$. Even the weak transitions between 20–25 kK are present in these three states. This similarity is a result of the same electron occupancy in the π space of the three cations and the small perturbation of the second unpaired electron occupying the nonbonding σ orbital of the $^3A''$ states of $C_{10}H_7$-$\alpha^+$ and $C_{10}H_7$-$\beta^+$ to the spectra. No transitions associated with this σ orbital were found because excitations of the π electrons to this orbital are symmetry forbidden.

The spectra of the neutral species, $C_{10}H_7$-$\alpha^{\cdot}$ and $C_{10}H_7$-$\beta^{\cdot}$, are also similar to the spectrum of naphthalene. A strong absorption resulting from the mixture of $\pi_4 \rightarrow \pi_6$ and $\pi_5 \rightarrow \pi_7$, was found near 43 kK for both compounds. A weak transition, $\pi_5 \rightarrow \pi_6$, was also found near 38 kK, slightly higher in energy than the corresponding peak of naphthalene.

In contrast to the close correspondence between the spectra of the cations and neutral compounds of the hydrogen abstracted derivatives and those of naphthalene, for the anions, $C_{10}H_7$-$\alpha^-$ and $C_{10}H_7$-$\beta^-$, the calculated spectra are not similar to that of the naphthalene anion. For example, no corresponding low-energy ($< 25$ kK) absorptions were found for these compounds. This is because, in the ground states $^1A'$, the extra electron occupies the nonbonding σ orbital of the carbon atom. As a result, the antibonding π or-

Table 5
INDO/S-CI calculated excited states of naphthalene cation (energy in 1000 $cm^{-1}$)

| State | This work [a] | | | Theory | | Experiment | | |
|---|---|---|---|---|---|---|---|---|
| | main configuration, coeff$^2$ | polarization | $\Delta E(f)$ | $\Delta E(f)$ [b] | $\Delta E(f)$ [c] | $\Delta E(f\times10^4)$ [d] | $\Delta E(f)$ [e] | $\Delta E(f)$ [f] |
| $1\,^2B_{3g}$ | $1b_{3g}\rightarrow1a_u$, 0.92 | $x$ | 15.2(0.105) | 21.5(0.20) | 14.4(0.091) | 14.8(4.0) | 14.5(0.04) | 14.8(0.20) |
| $1\,^2B_{2g}$ | $1a_u\rightarrow2b_{2g}$, 0.74; $1b_{3g}\rightarrow2b_{1u}$, 0.10 $2b_{1u}\rightarrow2b_{3g}$, 0.08 | $y$ | 20.5(0.040) | 32.6(0.01) | 22.7(0.115) | 21.9(0.2) | 21.4(0.01) | 21.0(0.08) |
| $2\,^2B_{2g}$ | $1b_{2g}\rightarrow1a_u$, 0.63; $2b_{1u}\rightarrow2b_{3g}$, 0.30 | $y$ | 25.0(0.068) | 35.6(0.22) | 19.2(0.006) | 26.5(1.0) | 25.8(0.03) | 26.0(0.30) |
| $2\,^2B_{3g}$ | $1a_u\rightarrow2b_{3g}$, 0.54; $2b_{1u}\rightarrow2b_{2g}$, 0.43 | $x$ | 34.6(0.017) | 33.3(0.02) | 34.4(0.195) | 32.4(8.0) | 32.5(0.05) | |
| $3\,^2B_{3g}$ | $2b_{1u}\rightarrow2b_{2g}$, 0.60; $1a_u\rightarrow2b_{3g}$, 0.26 $1a_u\rightarrow3b_{3g}$, 0.05 | $x$ | 36.7(0.492) | 45.6(1.92) | 37.3(0.363) | 36.2 | | |
| $3\,^2B_{2g}$ | $2b_{1u}\rightarrow2b_{3g}$, 0.49; $1b_{2g}\rightarrow1a_u$, 0.21 $2b_{1u}\rightarrow3b_{3g}$, 0.12; $1a_u\rightarrow2b_{2g}$, 0.10 | $y$ | 42.2(0.163) | | 43.9(0.100) | 40.9 | | |
| $4\,^2B_{2g}$ | $2b_{1u}\rightarrow2b_{3g}$, 0.90 | $y$ | 47.4(0.274) | | 52.3(0.363) | 44.9 | | |
| $4\,^2B_{3g}$ | $2b_{1u}\rightarrow2b_{2g}$, 0.50; $1a_u\rightarrow2b_{3g}$, 0.23 $1a_u\rightarrow2b_{3g}$, 0.16 | $x$ | 49.1(0.907) | | 49.3(0.977) | | | |

[a] CIS includes full 48 MOs of the ground state $^2A_u$ calculated with ROHF-SCF. Only allowed transitions are included.
[b] CNDO, Jorgensen and Poulsen, ref. [13].
[c] PPP, Zahradnik et al., ref. [14].
[d] Neon matrix, Salama and Allamandola, ref. [10].
[e] Freon matrix, Shita, ref. [16]. Oscillator strengths were converted from extinction coefficients with band widths of 1000 $cm^{-1}$.
[f] Polarized spectrum, Hiratsuka et al., ref. [17].

Table 6
INDO/S-CI calculated excited states of naphthalene anion (energy in 1000 $cm^{-1}$)

| State | This work [a] | | | Theory | | Experiment | | |
|---|---|---|---|---|---|---|---|---|
| | main configuration, coeff$^2$ | polarization | $\Delta E(f)$ | $\Delta E(f)$ [b] | $\Delta E(f)$ [c] | $\Delta E(f)$ [d] | $\Delta E(f)$ [e] | $\Delta E(f)$ [f] |
| $1\,^2B_{1u}$ | $2b_{2g}\rightarrow3b_{1u}$, 0.92 | $x$ | 9.7(0.066) | 16.2(0.16) | 14.1(0.970) | 11.9(0.02) | 11.8(0.02) | 12.2(0.01) |
| $1\,^2A_u$ | $2b_{2g}\rightarrow2a_u$, 0.82; $2b_{1u}\rightarrow2b_{3g}$, 0.08 | $y$ | 13.5(0.044) | 22.1(0.1) | 19.5(0.008) | 13.2(0.02) | 13.0(0.01) | |
| $2\,^2A_u$ | $1a_u\rightarrow2b_{2g}$, 0.69; $2b_{1u}\rightarrow2b_{3g}$, 0.14 $1b_{3g}\rightarrow3b_{1u}$, 0.08 | $y$ | 18.6(0.071) | 34.5(0.14) | 23.6(0.147) | 20.3(0.01) | 22.0(0.01) | |
| $1\,^2B_{3u}$ | $2b_{2g}\rightarrow\sigma^*_5$, 0.90 | $z$ | 33.7(0.032) | 36.5(0.00) | – | 27.0(0.03) | 27.0(0.03) | |
| $2\,^2B_{1u}$ | $1a_u\rightarrow2b_{3g}$, 0.68; $2b_{1u}\rightarrow2b_{2g}$, 0.27 | $x$ | 34.9(0.116) | 34.3(0.00) | 32.5(0.153) | 30.8(0.08) | 30.5(0.08) | 30.8(0.03) |
| $3\,^2B_{1u}$ | $2b_{1u}\rightarrow2b_{2g}$, 0.50; $1a_u\rightarrow2b_{3g}$, 0.40 | $x$ | 37.9(0.399) | 44.7(1.84) | 35.7(0.391) | 33.9(0.10) | 33.5(0.09) | 34.1(0.03) |
| $3\,^2A_u$ | $2b_{1u}\rightarrow2b_{3g}$, 0.62; $1a_u\rightarrow2b_{2g}$, 0.13 $2b_{1u}\rightarrow3b_{3g}$, 0.12; $2b_{2g}\rightarrow2a_u$, 0.09 | $y$ | 38.8(0.150) | – | 41.4(0.091) | | | |
| $2\,^2B_{3u}$ | $2b_{2g}\rightarrow\sigma^*_6$, 0.88; $2b_{1u}\rightarrow\sigma^*_7$, 0.05 | $z$ | 45.7(0.008) | 40.7(0.00) | – | | | |
| $4\,^2A_u$ | $2b_{1u}\rightarrow2b_{3g}$, 0.91 | $y$ | 45.4(0.235) | | 44.4(0.919) | | 43.5(0.16) | 43.0(0.03) |
| $4\,^2B_{1u}$ | $1a_u\rightarrow2b_{3g}$, 0.77; $2b_{1u}\rightarrow2b_{2g}$, 0.16 | $x$ | 49.3(0.847) | | | | | |

[a] CIS includes full 48 MOs of the ground state $^2B_{2g}$ calculated with ROHF-SCF. Only allowed transitions are included.
[b] CNDO, Jorgensen and Poulsen, ref. [13].
[c] PPP, Heinze and Zimmermann, ref. [15].
[d] MTHF, Shida, ref. [9]. Oscillator strengths were converted from extinction coefficients with band widths of 1000 $cm^{-1}$.
[e] Solution, Brandes and Gerdes, ref. [18]. Oscillator strengths were converted from extinction coefficients with band widths of 1000 $cm^{-1}$.
[f] Glass, Hoijtink and Zandstra, ref. [30]. Oscillator strengths were converted from extinction coefficients with band widths of 1000 $cm^{-1}$.

Table 7
Calculated spectrum of $C_{10}H_7$-a$^+$ ($^3$A″)

| State | $E$ (kK) | $f$ | Polarization | Excitation | | Coeff$^2$ |
|---|---|---|---|---|---|---|
| 3 $^3$A″ | 16.1 | 0.094 | $x$ | 3a″ (pi3) | −5a″ (pi5) | 0.89 |
| 4 $^3$A″ | 21.9 | 0.030 | $y$ | 5a″ (pi5) | −6a″ (pi6) | 0.69 |
| | | | | 3a″ (pi3) | −8a″ (pi8) | 0.11 |
| | | | | 4a″ (pi4) | −7a″ (pi7) | 0.10 |
| 1 $^3$A′ | 24.9 | 0.004 | $z$ | 19a′ (Casp2) | −6a″ (pi6) | 0.67 |
| | | | | 19a′ (Casp2) | −8a″ (pi8) | 0.14 |
| 5 $^3$A″ | 25.0 | 0.034 | $y$ | 2a″ (pi2) | −5a″ (pi5) | 0.52 |
| | | | | 4a″ (pi4) | −7a″ (pi7) | 0.38 |
| 6 $^3$A″ | 27.0 | 0.014 | $y$ | 4a″ (pi4) | −7a″ (pi7) | 0.69 |
| | | | | 2a″ (pi2) | −5a″ (pi5) | 0.10 |
| 7 $^3$A″ | 30.0 | 0.009 | $x$ | 4a″ (pi4) | −6a″ (pi6) | 0.75 |
| 8 $^3$A″ | 31.1 | 0.003 | $x$ | 5a″ (pi5) | −8a″ (pi8) | 0.45 |
| | | | | 3a″ (pi3) | −6a″ (pi6) | 0.20 |
| | | | | 4a″ (pi4) | −6a″ (pi6) | 0.16 |
| 10 $^3$A″ | 34.3 | 0.009 | $x$ | 5a″ (pi5) | −7a″ (pi7) | 0.56 |
| | | | | 4a″ (pi4) | −6a″ (pi6) | 0.29 |
| 4 $^3$A′ | 35.3 | 0.001 | $z$ | 3a″ (pi3) | −19a′ (Casp2) | 0.84 |
| 11 $^3$A″ | 37.2 | 0.053 | $x$ | 4a″ (pi4) | −8a″ (pi8) | 0.40 |
| | | | | 3a″ (pi3) | −7a′ (pi7) | 0.25 |
| | | | | 4a″ (pi4) | −6a″ (pi6) | 0.15 |
| | | | | 2a″ (pi2) | −6a″ (pi6) | 0.10 |
| 12 $^3$A″ | 37.7 | 0.509 | $x$ | 4a″ (pi4) | −6a″ (pi6) | 0.58 |
| | | | | 5a″ (pi5) | −7a″ (pi7) | 0.17 |

Table 8
Calculated spectrum of $C_{10}H_7$-a$^-$ ($^2$A′)

| State | $E$ (kK) | $f$ | Polarization | Excitation | | Coeff$^2$ |
|---|---|---|---|---|---|---|
| 2 $^2$A″ | 27.3 | 0.007 | $z$ | 19a′ (Casp2) | −6a″ (pi6) | 0.53 |
| | | | | 19a′ (Casp2) | −8a″ (pi8) | 0.16 |
| | | | | 5a″ (pi5) | −19a′ (Casp2) | 0.11 |
| 6 $^2$A′ | 31.9 | 0.008 | $x$ | 5a″ (pi5) | −7a″ (pi7) | 0.40 |
| | | | | 4a″ (pi4) | −6a″ (pi6) | 0.28 |
| | | | | 5a″ (pi5) | −9a″ (pi9) | 0.11 |
| 8 $^2$A′ | 34.2 | 0.008 | $xy$ | 4a″ (pi4) | −6a″ (pi6) | 0.44 |
| | | | | 5a″ (pi5) | −9a″ (pi9) | 0.18 |
| | | | | 5a″ (pi5) | −7a″ (pi7) | 0.14 |
| 9 $^2$A′ | 36.9 | 0.153 | $y$ | 5a″ (pi5) | −6a″ (pi6) | 0.89 |
| | | | | 4a″ (pi4) | −7a″ (pi7) | 0.08 |

bitals are left unoccupied, which is exactly the same electron configuration of the neutral naphthalene. In fact, the spectra of $C_{10}H_7$-$\alpha^-$ and $C_{10}H_7$-$\beta^-$ are similar in some aspects to that of naphthalene.

The calculated spectra of the hydrogen addition derivatives vary according to the position of hydrogen addition. Because of the disruption of the aromatic conjugation in the π space, they do not resemble naphthalene and its ions. Among the different ionization states of these derivatives, the anions tend to have stronger absorptions near 20 kK and the cation have stronger transitions near 30 kK. Only weak transitions were found for the neutral compounds in these two regions.

These calculated spectra of naphthalene derivatives can be useful in identifying extra absorptions

Table 9
Calculated spectrum of $C_{10}H_7$-a$^-$ ($^1$A′)

| State | $E$ (kK) | $f$ | Polarization | Excitation | Coeff$^2$ |
|---|---|---|---|---|---|
| 1 $^1$A″ | 9.9 | 0.004 | $z$ | 19a′ (Casp2)–6a″ (pi6) | 0.67 |
| | | | | 19a′ (Casp2)–9a″ (pi9) | 0.13 |
| | | | | 19a′ (Casp2)–10a″ (pi10) | 0.12 |
| 3 $^1$A″ | 23.5 | 0.002 | $z$ | 19a′ (Casp2)–8a″ (pi8) | 0.41 |
| | | | | 19a′ (Casp2)–6a″ (pi6) | 0.28 |
| | | | | 19a′ (Casp2)–10a″ (pi10) | 0.19 |
| | | | | 19a′ (Casp2)–9a″ (pi9) | 0.11 |
| 4 $^1$A″ | 31.3 | 0.009 | $z$ | 19a′ (Casp2)–8a″ (pi8) | 0.42 |
| | | | | 19a′ (Casp2)–10a″ (pi10) | 0.25 |
| | | | | 19a′ (Casp2)–9a″ (pi9) | 0.19 |
| | | | | 19a′ (Casp2)–7a″ (pi7) | 0.10 |
| 2 $^1$A′ | 30.5 | 0.093 | $xy$ | 5a″ (pi5) –6a″ (pi6) | 0.71 |
| | | | | 5a″ (pi5) –7a″ (pi7) | 0.14 |
| 3 $^1$A′ | 31.9 | 0.042 | $xy$ | 5a″ (pi5) –7a″ (pi7) | 0.47 |
| | | | | 4a″ (pi4) –6a″ (pi6) | 0.28 |
| | | | | 5a″ (pi5) –6a″ (pi6) | 0.19 |
| 4 $^1$A′ | 36.4 | 0.005 | $xy$ | 19a′ (Casp2)–20a′ | 0.58 |
| | | | | 19a′ (Casp2)–22a′ | 0.26 |

observed in the laboratory. For example, absorptions of the naphthalene anion observed in the 20–25 kK region were first attributed to hydrogen adduct impurities based on the observation that these transitions are non-polarized [20,31]. However, these two transitions were reassigned to the transitions of naphthalene anion itself by Shida and Iwata [16]. According to the current results, the naphthalene anion is not predicted to have observable transitions in this region. Instead, the hydrogen addition derivatives, $C_{10}H_9$-$\beta^-$ and $C_{10}H_9$-$\alpha^-$ for example, show weak and moderate absorption in this region.

## 5. Relevance to the diffuse interstellar bands (DIBs) issue

The calculated electronic transitions of naphthalene and its neutral and ionic derivatives relevant to the DIBs, are reported in table 19. From the astrophysical point of view, these calculations indicate that:

(1) Neutral naphthalene and its dehydrogenated counterparts ($C_{10}H_7$-$\alpha$ and $C_{10}H_7$-$\beta$) do not absorb in the visible region and, hence, cannot contribute to the DIBs. On the contrary, the neutral species $C_{10}H_9$-$\alpha$ and $C_{10}H_9$-$\beta$ do show electronic absorptions in the visible region, and could contribute to the DIBs.

(2) Naphthalene anion and its derivatives obtained either by abstraction or addition of a hydrogen atom all show electronic transitions falling in the visible or/and near-infrared regions, implying possible contributions to the DIBs.

(3) Naphthalene cation and its dehydrogenated counterparts ($C_{10}H_{-7}$-$\alpha^+$ and $C_{10}H_{-7}$-$\beta^+$) do absorb in the visible region and, hence, could contribute to the DIBs. $C_{10}H_9$-$\alpha^+$ and $C_{10}H_9$-$\beta^+$, however, do not absorb in the visible region and cannot contribute to the DIBs.

In all, 19 electronic transitions of naphthalene and its derivatives fall in the range of the diffuse interstellar bands designating these species as potential candidates for the DIBs, as shown in table 19.

One should, however, bear in mind two important facts when making such correlations. First, theoretical calculations provide the relative energies of the electronic levels of each molecular species and, hence, these values can be shifted from the absolute values measured experimentally and which can be correlated to the DIBs. For example, in the case of the naphthalene cation ($C_{10}H_8^+$), a comparison of the calculated energy levels with the corresponding values measured when the molecular ion is isolated in a neon matrix [10,11], which constitutes the most relevant environment to simulate the conditions reign-

Table 10
Calculated spectrum of $C_{10}H_7$-b$^+$ ($^3$A″)

| State | $E$ (kK) | $f$ | Polarization | Excitation | Coeff$^2$ |
|---|---|---|---|---|---|
| 3 $^3$A″ | 16.2 | 0.095 | $x$ | 3a″ (pi3) −5a″ (pi5) | 0.89 |
| 4 $^3$A′ | 21.7 | 0.030 | $y$ | 5a″ (pi5) −6a″ (pi6) | 0.72 |
| | | | | 3a″ (pi3) −8a″ (pi8) | 0.11 |
| 1 $^3$A′ | 24.2 | 0.002 | $z$ | 19a′ (Cbsp2) −6a″ (pi6) | 0.40 |
| | | | | 4a″ (pi4) −19a′ (Cbsp2) | 0.16 |
| | | | | 19a′ (Cbsp2) −7a″ (pi7) | 0.11 |
| | | | | 19a′ (Cbsp2) −9a″ (pi9) | 0.10 |
| | | | | 19a′ (Cbsp2) −8a″ (pi8) | 0.10 |
| 5 $^3$A″ | 25.1 | 0.049 | $y$ | 2a″ (pi2) −5a″ (pi5) | 0.59 |
| | | | | 4a″ (pi4) −7a″ (pi7) | 0.34 |
| 6 $^3$A″ | 26.2 | 0.001 | $xy$ | 4a″ (pi4) −7a″ (pi7) | 0.63 |
| | | | | 4a″ (pi4) −6a″ (pi6) | 0.11 |
| | | | | 3a″ (pi3) −8a″ (pi8) | 0.10 |
| 7 $^3$A″ | 29.2 | 0.001 | $xy$ | 4a″ (pi4) −6a″ (pi6) | 0.54 |
| | | | | 3a″ (pi3) −6a″ (pi6) | 0.28 |
| 8 $^3$A″ | 30.2 | 0.001 | $xy$ | 5a″ (pi5) −8a″ (pi8) | 0.57 |
| | | | | 3a″ (pi3) −6a″ (pi6) | 0.20 |
| 10 $^3$A″ | 34.6 | 0.036 | $x$ | 5a″ (pi5) −7a″ (pi7) | 0.54 |
| | | | | 4a″ (pi4) −6a″ (pi6) | 0.40 |
| 11 $^3$A″ | 35.9 | 0.047 | $x$ | 4a″ (pi4) −8a″ (pi8) | 0.49 |
| | | | | 3a″ (pi3) −7a″ (pi7) | 0.20 |
| | | | | 2a″ (pi2) −6a″ (pi6) | 0.11 |
| 12 $^3$A″ | 37.4 | 0.433 | $x$ | 4a″ (pi4) −6a″ (pi6) | 0.55 |
| | | | | 5a″ (pi5) −7a″ (pi7) | 0.19 |
| 2 $^3$A′ | 28.4 | 0.003 | $z$ | 4a″ (pi4) −19a′ (Cbsp2) | 0.54 |
| | | | | 19a′ (Cbsp2) −6a″ (pi6) | 0.18 |
| | | | | 2a″ (pi2) −19a′ (Cbsp2) | 0.15 |
| 4 $^3$A′ | 34.0 | 0.004 | $z$ | 19a′ (Cbsp2) −7a″ (pi7) | 0.51 |
| | | | | 19a′ (Cbsp2) −9a″ (pi9) | 0.16 |
| | | | | 19a′ (Cbsp2) −6a″ (pi6) | 0.14 |

ing in the interstellar medium (i.e. the least perturbing medium), indicates shifts of about 400 cm$^{-1}$ (162 Å at ≈6500 Å) and 1400 cm$^{-1}$ (318 Å at ≈4500 Å) for the two visible transitions falling in the range of the DIBs (see tables 5 and 19). This implies that one needs to deal carefully with such results which must be used only as a tool to preselect plausible candidates for the DIBs and help focus on the species which deserve an experimental study. Second, these calculations provide the electronic energy levels of naphthalene and its derivatives but no information on the vibronic structure which is part of the real spectrum, was included. The vibronic structure is particularly important here to explain the interstellar features as indicated by the case of the naphthalene cation ($C_{10}H_8^+$) where all the 6 visible bands which do fit DIBs belong to the same electronic band system (the lowest energy system at 6579 Å (theory)/6741 Å (Ne matrix)) [10,11]. The vibronic structure will be obtained from the laboratory measurement of the spectra of the species preselected from the theoretical calculations.

Finally, it can be seen how important is the role of theoretical calculations to help clarify a problem as complex as the identification of the DIBs. Faced with a large family of molecules (PAHs) including numerous isomers which can each show multiple possibilities for hydrogen-atom addition or abstraction and need to be considered in their neutral and ionized forms, one is faced with an enormous (if not impossible) task to test the relevance of each candidate to the DIBs. Theoretical calculations of the electronic structures of a vast number of these species allow one to preselect potential candidates for labora-

Table 11
Calculated spectrum of $C_{10}H_7$-b· ($^2A'$)

| State | $E$ (kK) | $f$ | Polarization | Excitation | Coeff$^2$ |
|---|---|---|---|---|---|
| $2\,^2A''$ | 28.5 | 0.006 | $z$ | 19a′ (Cbsp2) –6a″ (pi6) | 0.38 |
| | | | | 19a′ (Cbsp2) –7a″ (pi7) | 0.16 |
| | | | | 5a″ (pi5) –19a′ (Cbsp2) | 0.13 |
| | | | | 19a′ (Cbsp2) –9a″ (pi9) | 0.11 |
| | | | | 19a′ (Cbsp2) –8a″ (pi8) | 0.11 |
| $5\,^2A'$ | 29.5 | 0.001 | $y$ | 4a″ (pi4) –7a″ (pi7) | 0.66 |
| | | | | 5a″ (pi5) –6a″ (pi6) | 0.14 |
| $6\,^2A'$ | 32.4 | 0.005 | $xy$ | 5a″ (pi5) –7a″ (pi7) | 0.41 |
| | | | | 4a″ (pi4) –6a″ (pi6) | 0.35 |
| $7\,^2A'$ | 33.7 | 0.005 | $xy$ | 4a″ (pi4) –6a″ (pi6) | 0.54 |
| | | | | 5a″ (pi5) –7a″ (pi7) | 0.28 |
| $8\,^2A'$ | 34.5 | 0.009 | $y$ | 5a″ (pi5) –7a″ (pi7) | 0.28 |
| | | | | 5a″ (pi5) –9a″ (pi9) | 0.22 |
| | | | | 4a″ (pi4) –8a″ (pi8) | 0.18 |
| | | | | 2a″ (pi2) –6a″ (pi6) | 0.11 |
| $4\,^2A''$ | 34.9 | 0.002 | $z$ | 19a′ (Cbsp2) –7a″ (pi7) | 0.44 |
| | | | | 19a′ (Cbsp2) –6a″ (pi6) | 0.24 |
| | | | | 19a′ (Cbsp2) –9a″ (pi9) | 0.11 |
| $9\,^2A'$ | 37.0 | 0.161 | $y$ | 5a″ (pi5) –6a″ (pi6) | 0.84 |

Table 12
Calculated spectrum of $C_{10}H_7$-b$^-$ ($^1A'$)

| State | $E$ (kK) | $f$ | Polarization | Excitation | Coeff$^2$ |
|---|---|---|---|---|---|
| $1\,^1A''$ | 9.6 | 0.001 | $z$ | 19a′ (Cbsp2) –6a″ (pi6) | 0.66 |
| | | | | 19a′ (Cbsp2) –8a″ (pi8) | 0.26 |
| $2\,^1A''$ | 14.7 | 0.004 | $z$ | 19a′ (Cbsp2) –7a″ (pi7) | 0.60 |
| | | | | 19a′ (Cbsp2) –9a″ (pi9) | 0.20 |
| | | | | 19a′ (Cbsp2) –10a″ (pi10) | 0.16 |
| $3\,^1A''$ | 25.1 | 0.003 | $z$ | 19a′ (Cbsp2) –8a″ (pi8) | 0.62 |
| | | | | 19a′ (Cbsp2) –6a″ (pi6) | 0.30 |
| $2\,^1A'$ | 30.0 | 0.100 | $xy$ | 5a″ (pi5) –6a″ (pi6) | 0.78 |
| $4\,^1A''$ | 30.6 | 0.012 | $z$ | 19a′ (Cbsp2) –10a″ (pi10) | 0.51 |
| | | | | 19a′ (Cbsp2) –7a″ (pi7) | 0.32 |
| | | | | 19a′ (Cbsp2) –8a″ (pi8) | 0.10 |
| $3\,^1A'$ | 33.1 | 0.015 | $xy$ | 5a″ (pi5) –7a″ (pi7) | 0.47 |
| | | | | 4a″ (pi4) –6a″ (pi6) | 0.33 |
| | | | | 5a″ (pi5) –6a″ (pi6) | 0.12 |
| $4\,^1A'$ | 35.4 | 0.045 | $x$ | 19a′ (Cbsp2) –20a′ | 0.41 |
| | | | | 19a′ (Cbsp2) –21a′ | 0.26 |

Table 13
Calculated spectrum of $C_{10}H_9$-a$^+$ ($^1A'$)

| State | $E$ (kK) | $f$ | Polarization | Excitation | Coeff$^2$ |
|---|---|---|---|---|---|
| $2\,^1A'$ | 25.8 | 0.077 | $xy$ | 5a″ (pi4)–6a″ (pi5) | 0.97 |
| $3\,^1A'$ | 29.0 | 0.489 | $x$ | 4a″ (pi3)–6a″ (pi5) | 0.95 |

Table 14
Calculated spectrum of $C_{10}H_9$-a· ($^2A''$)

| State | $E$ (kK) | $f$ | Polarization | Excitation | Coeff$^2$ |
|---|---|---|---|---|---|
| $2\,^2A''$ | 15.7 | 0.001 | $x$ | 6a″ (pi5)–7a″ (pi6) | 0.43 |
| | | | | 4a″ (pi3)–6a″ (pi5) | 0.16 |
| | | | | 5a″ (pi4)–8a″ (pi7) | 0.10 |
| $3\,^2A''$ | 23.4 | 0.006 | $xy$ | 6a″ (pi5)–8a″ (pi7) | 0.29 |
| | | | | 6a″ (pi5)–9a″ (pi8) | 0.19 |
| | | | | 4a″ (pi3)–8a″ (pi7) | 0.10 |
| | | | | 5a″ (pi4)–6a″ (pi5) | 0.10 |
| $4\,^2A''$ | 23.6 | 0.002 | $xy$ | 6a″ (pi5)–9a″ (pi8) | 0.26 |
| | | | | 6a″ (pi5)–8a″ (pi7) | 0.19 |
| | | | | 4a″ (pi3)–7a″ (pi6) | 0.10 |
| $5\,^2A''$ | 30.8 | 0.014 | $xy$ | 5a″ (pi4)–8a″ (pi7) | 0.49 |
| | | | | 5a″ (pi4)–6a″ (pi5) | 0.13 |
| $1\,^2A'$ | 34.0 | 0.001 | $z$ | 6a″ (pi5)–20a′ | 0.77 |
| $2\,^2A''$ | 34.6 | 0.027 | $y$ | 5a″ (pi4)–6a″ (pi5) | 0.25 |
| | | | | 5a″ (pi4)–7a″ (pi6) | 0.17 |
| | | | | 5a″ (pi4)–8a″ (pi7) | 0.16 |
| | | | | 6a″ (pi5)–8a″ (pi7) | 0.14 |
| $7\,^2A''$ | 36.4 | 0.239 | $x$ | 4a″ (pi3)–6a″ (pi5) | 0.44 |
| | | | | 6a″ (pi5)–7a″ (pi6) | 0.27 |
| $2\,^2A'$ | 39.4 | 0.002 | $z$ | 6a″ (pi5)–21a′ | 0.53 |
| | | | | 6a″ (pi5)–23a′ | 0.21 |
| | | | | 4a″ (pi3)–20a′ | 0.10 |

Table 15
Calculated spectrum of $C_{10}H_9$-a$^-$ ($^1A'$)

| State | $E$ (kK) | $f$ | Polarization | Excitation | Coeff$^2$ |
|---|---|---|---|---|---|
| $2\,^1A'$ | 20.0 | 0.025 | $xy$ | 6a″ (pi5)–7a″ (pi6) | 0.57 |
| | | | | 6a″ (pi5)–8a″ (pi7) | 0.39 |
| $3\,^1A'$ | 22.1 | 0.417 | $x$ | 6a″ (pi5)–8a″ (pi7) | 0.54 |
| | | | | 6a″ (pi5)–7a″ (pi6) | 0.40 |
| $4\,^1A'$ | 34.9 | 0.172 | $y$ | 6a″ (pi5)–22a′ | 0.47 |
| $3\,^1A''$ | 39.3 | 0.002 | $z$ | 6a″ (pi5)–24a′ | 0.31 |
| | | | | 6a″ (pi5)–21a′ | 0.18 |

Table 16
Calculated spectrum of $C_{10}H_9$-b$^+$ ($^1A'$)

| State | $E$ (kK) | $f$ | Polarization | Excitation | Coeff$^2$ |
|---|---|---|---|---|---|
| $2\,^1A'$ | 23.4 | 0.184 | $xy$ | 5a″ (pi4)–6a″ (pi5) | 0.97 |
| $3\,^1A'$ | 35.6 | 0.138 | $xy$ | 4a″ (pi3)–6a″ (pi5) | 0.69 |
| | | | | 5a″ (pi4)–7a″ (pi6) | 0.26 |
| $4\,^1A'$ | 40.0 | 0.014 | $xy$ | 3a″ (pi2)–6a″ (pi5) | 0.73 |
| | | | | 5a″ (pi4)–8a″ (pi7) | 0.13 |

Table 17
Calculated spectrum of $C_{10}H_9$-b· ($^2A''$)

| State | $E$ (kK) | $f$ | Polarization | Excitation | Coeff$^2$ |
|---|---|---|---|---|---|
| $2\,^2A''$ | 13.3 | 0.001 | $xy$ | 5a″ (pi4)–7a″ (pi6) | 0.32 |
| | | | | 6a″ (pi5)–7a″ (pi6) | 0.26 |
| $3\,^2A''$ | 18.4 | 0.006 | $xy$ | 6a″ (pi5)–8a″ (pi7) | 0.30 |
| | | | | 4a″ (pi4)–8a″ (pi7) | 0.29 |
| | | | | 4a″ (pi3)–6a″ (pi5) | 0.11 |
| $4\,^2A''$ | 22.8 | 0.001 | $y$ | 6a″ (pi5)–9a″ (pi8) | 0.19 |
| | | | | 5a″ (pi4)–9a″ (pi8) | 0.15 |
| | | | | 6a″ (pi5)–7a″ (pi6) | 0.12 |
| $5\,^2A''$ | 28.5 | 0.087 | $xy$ | 5a″ (pi4)–8a″ (pi7) | 0.37 |
| | | | | 5a″ (pi4)–6a″ (pi5) | 0.29 |
| | | | | 6a″ (pi5)–7a″ (pi6) | 0.10 |
| $6\,^2A''$ | 30.6 | 0.040 | $xy$ | 5a″ (pi4)–7a″ (pi6) | 0.33 |
| | | | | 6a″ (pi5)–7a″ (pi6) | 0.12 |
| | | | | 4a″ (pi3)–7a″ (pi6) | 0.11 |
| | | | | 5a″ (pi4)–9a″ (pi8) | 0.11 |
| $1\,^2A'$ | 33.7 | 0.004 | $z$ | 6a″ (pi5)–20a′ | 0.70 |
| $7\,^2A''$ | 35.0 | 0.005 | $xy$ | 6a″ (pi5)–9a″ (pi9) | 0.21 |
| | | | | 4a″ (pi3)–9a″ (pi9) | 0.15 |
| | | | | 6a″ (pi5)–9a″ (pi8) | 0.11 |
| $8\,^2A''$ | 38.8 | 0.030 | $y$ | 5a″ (pi4)–8a″ (pi7) | 0.25 |
| | | | | 5a″ (pi4)–7a″ (pi6) | 0.20 |
| | | | | 4a″ (pi3)–6a″ (pi5) | 0.15 |

Table 18
Calculated spectrum of $C_{10}H_9$-b$^-$ ($^1A'$)

| State | $E$ (kK) | $f$ | Polarization | Excitation | Coeff$^2$ |
|---|---|---|---|---|---|
| $2\,^1A'$ | 16.4 | 0.108 | $xy$ | 6a″ (pi5)–7a″ (pi6) | 0.98 |
| $3\,^1A'$ | 26.8 | 0.037 | $xy$ | 6a″ (pi5)–9a″ (pi8) | 0.67 |
| | | | | 6a″ (pi5)–8a″ (pi7) | 0.30 |
| $4\,^1A'$ | 29.9 | 0.375 | $xy$ | 6a″ (pi5)–8a″ (pi7) | 0.61 |
| | | | | 6a″ (pi5)–9a″ (pi8) | 0.31 |
| $2\,^1A''$ | 37.0 | 0.003 | $z$ | 6a″ (pi5)–21a′ | 0.84 |

tory study to be performed in an environment relevant to astrophysical applications. Then, and only then, can a one-to-one correspondence between the measured spectra of PAH derivatives and the DIBs be attempted.

## 6. Conclusions

Comparison of the calculated spectra with experiment shows that the optical spectra of naphthalene and its ions can be reliably predicted by the INDO/S method. The degree of similarity of the predicted spectra of the hydrogen abstraction and derivatives to those of naphthalene and ions depends largely on the similarity of the $\pi$ electron configurations. For the hydrogen addition derivatives, very little resemblance of the predicted spectra to naphthalene was found because of the disruption of the aromatic conjugation system.

The study of the astrophysical implications of this work indicates that 19 electronic transitions of naphthalene and its derivatives fall in the visible and near-infrared range suggesting a possible correlation with the diffuse interstellar bands (DIBs). The selected species, reported in table 19, are tentatively desig-

Table 19
Calculated energies and oscillator strengths of electronic transitions of naphthalene and derivatives relevant to the DIB issue

| Energy ($cm^{-1}$) | Wavelength (Å) | Oscillator strength | Species |
|---|---|---|---|
| 15 200 | 6 579 | 0.105 | $C_{10}H_8^+$ |
| 20 500 | 4 878 | 0.040 | $C_{10}H_8^+$ |
| 9 700 | 10 309 | 0.066 | $C_{10}H_8^-$ |
| 13 500 | 7 407 | 0.044 | $C_{10}H_8^-$ |
| 18 600 | 5 376 | 0.071 | $C_{10}H_8^-$ |
| 16 100 | 6 211 | 0.094 | $C_{10}H_7$-$\alpha^+$ |
| 21 900 | 4 566 | 0.030 | $C_{10}H_7$-$\alpha^+$ |
| 9 900 | 10 101 | 0.004 | $C_{10}H_7$-$\alpha^-$ |
| 16 200 | 6 173 | 0.095 | $C_{10}H_7$-$\beta^+$ |
| 21 700 | 4 608 | 0.030 | $C_{10}H_7$-$\beta^+$ |
| 9 600 | 10 417 | 0.001 | $C_{10}H_7$-$\beta^-$ |
| 14 700 | 6 803 | 0.004 | $C_{10}H_7$-$\beta^-$ |
| 15 700 | 6 369 | 0.001 | $C_{10}H_9$-$\alpha$ |
| 20 000 | 5 000 | 0.025 | $C_{10}H_9$-$\alpha^-$ |
| 22 100 | 4 525 | 0.417 | $C_{10}H_9$-$\alpha^-$ |
| 13 300 | 7 519 | 0.001 | $C_{10}H_9$-$\beta$ |
| 18 400 | 5 435 | 0.006 | $C_{10}H_9$-$\beta$ |
| 22 800 | 4 836 | 0.001 | $C_{10}H_9$-$\beta$ |
| 16 400 | 6 098 | 0.108 | $C_{10}H_9$-$\beta^-$ |

nated as potential candidates for some of the DIBs, since the calculated wave lengths are in the same region. However, it is stressed that further experimental studies in an astrophysically relevant environment are needed to establish a definitive one-to-one correlation between the vibronic bands of a given PAH species and some of the DIBs.

## Acknowledgement

This work is supported by NASA–Ames Cooperative Agreement Number NCC 2-733. We acknowledge several important discussions with Lou Allamandola regarding the astrophysical implications of this study.

## References

[1] Nato Advanced Research and Workshop on Polycyclic Aromatic Hydrocarbons and Astrophysics (Reidel, Dordrecht, 1987).
[2] L.J. Allamandola, A. Tielens and J.R. Barker, Astrophys. J. Suppl. Ser. 71 (1989) 733.
[3] L.J. Allamandola, in: Current chemistry, eds. S. Cyvin and J. Gutman (Springer, Berlin, 1990).
[4] J.L. Puget and A. Leger, Ann. Rev. Astron. Astrophys. 27 (1989) 161.
[5] G.P. Van der Zwet and L.J. Allamandola, Astron. Astrophys. 146 (1985) 76;
A. Léger and L.B. d'Hendecourt, Astron. Astrophys. 146 (1985) 81;
M.K. Crawford, A.G.G.M. Tielens and L.J. Allamandola, Astrophys. J. 293 (1985) L45.
[6] G.H. Herbig, Astrophys. J. 196 (1975) 129; 331 (1988) 999; 382 (1991) 193.
[7] L.A. Nakhimovsky, M. Lamotte and J. Joussot-Dubien, Handbook of low temperature electronic spectra of polycyclic aromatic hydrocarbons (Elsevier, Amsterdam, 1989).
[8] Spectral atlas of polycyclic aromatic compounds (Reidel, Dordrecht, 1985).
[9] T. Shida, Electronic absorption spectra of radical ions (Elsevier, Amsterdam, 1988).
[10] F. Salama and L.J. Allamandola, J. Chem. Phys. 94 (1991) 6964.
[11] F. Salama and L.J. Allamandola, Astrophys. J. 395 (1992) 301.
[12] R. Pariser, J. Chem. Phys. 24 (1956) 250;
B. Roos and P.N. Skancke, Acta Chem. Scand. 21 (1967) 233;
P. Tavan and K. Shulten, J. Chem. Phys. 70 (1979) 5414.
[13] P. Jorgensen and J.C. Poulsen, J. Phys. Chem. 78 (1974) 1420.

[14] R. Zahradnik, P. Carsky and Z. Slanina, Collect. Czech. Chem. Commun. 38 (1973) 1886.
[15] J. Heinze and H.W. Zimmermann, Ber. Bunsenges. Physik. Chem. 81 (1977) 321.
[16] T. Shida and S. Iwata, J. Am. Chem. Soc. 95 (1973) 3473.
[17] H. Hiratzuka, Can. J. Chem. 65 (1987) 1185.
[18] K.K. Brandes and R.J. Gerdes, J. Phys. Chem. 71 (1967) 508.
[19] G.J. Hoijtink, N.H. Velthorst and P.J. Zandstra, Mol. Phys. 3 (1960) 533.
[20] G.J. Hoijtink, Mol. Phys. 2 (1959) 85.
[21] MOPAC: QCPE Program No. 455 (5.0).
[22] M.J.S. Dewar, E.G. Zoebisch, E.F. Healy and J.J.P. Stewart, J. Am. Chem. Soc. 107 (1985) 3902.
[23] M.C. Zerner, G.H. Loew, R. Kirchner and U.T. Muller-Westerhoff, J. Am. Chem. Soc. 102 (1980) 589.
[24] L. Pauling, Acta Cryst. B 36 (1980) 1898.
[25] M.C. Zerner, Intern. J. Quantum Chem. 35 (1989) 567.
[26] J.E. Ridley and M.C. Zerner, J. Mol. Spectry. 50 (1974) 457.
[27] S. Canuto and M.C. Zerner, Astrophys. J. 377 (1991) 150.
[28] R.H. Huebner, S.R. Mielczarek and C.E. Kuyatt, Chem. Phys. Letters 16 (1972) 464.
[29] G.A. George and G.C. Morris, J. Mol. Spectry. 26 (1968) 647.
[30] J.M.O. Matos and B.O. Roos, Theoret. Chim. Acta 74 (1988) 363.
[31] G.J. Hoijtink and P.J. Zandstra, Mol. Phys. 3 (1960) 371.